SCIENCE CHINA
Information Sciences

• RESEARCH PAPER •

August 2016, Vol. 59 082304:1–082304:16
doi: 10.1007/s11432-015-5476-6

Performance analysis of MIMO systems with arbitrary number transmit antenna selection and OSTBC in the presence of imperfect CSI

Xiangbin YU[1,2*], Xiang-Gen XIA[2] & Shuhung LEUNG[3,4]

[1]*Department of Electronic Engineering, Nanjing University of Aeronautics and Astronautics, Nanjing* 210016*, China;*
[2]*Department of Electrical and Computer Engineering, University of Delaware, Delaware* 19716*, USA;*
[3]*Department of Electronic Engineering, City University of Hong Kong, Hong Kong, China;*
[4]*State Key Laboratory of Millimeter Waves, City University of Hong Kong, Hong Kong, China*

Received July 8, 2015; accepted August 30, 2015; published online April 8, 2016

Abstract In this paper, the performance analysis of MIMO systems with arbitrary number transmit antenna selection (TAS) and orthogonal space-time block coding (STBC) in Rayleigh fading channels for imperfect channel state information (CSI) is presented. For the performance analysis, the moment generating function of the system effective SNR as well as its upper and lower bounds are derived. Then, accurate and approximate expressions of bit error rate (BER) of MIMO-TAS-STBC with MPSK and MQAM are further derived. Using the approximate BER formula and imperfect CSI, an adaptive antenna selection scheme is developed for minimizing the BER. The diversity gain and coding gain are analyzed at high SNR. The results indicate that the MIMO-TAS-STBC for imperfect CSI can only achieve partial diversity order KN and the coding gain is affected by K, N, code rate, modulation pattern, and channel correlation coefficients, when K transmit antennas are selected and N receive antennas are used. Simulation results show that the theoretical analysis matches the simulation result well, and the approximate expressions are close to the accurate ones but have a lower complexity.

Keywords MIMO, arbitrary number antenna selection, imperfect CSI, space-time block coding, diversity gain, bit error rate.

Citation Yu X B, Xia X-G, Leung S H. Performance analysis of MIMO systems with arbitrary number transmit antenna selection and OSTBC in the presence of imperfect CSI. Sci China Inf Sci, 2016, 59(8): 082304, doi: 10.1007/s11432-015-5476-6

1 Introduction

It is well-known that for a multi-input and multi-output (MIMO) system, either space-time coding or antenna selection can achieve spatial diversity, see for example [1–8]. When multiple transmit antennas are selected, applying space-time coding to selected transmit antennas may improve the system performance further [9–18].

By employing transmit antenna selection (TAS) technique, the error rate performances of MIMO systems have been studied in [5–16]. Selecting one transmit antenna is studied in [5,6] for MIMO systems,

* Corresponding author (email: yxbxwy@gmail.com)

in [7] for multi-user relay networks and in [8] for wiretap channels, etc. Selecting two and three transmit antennas are studied in [9] and [10], respectively, for MIMO systems with STBC. With selecting multiple transmit antennas, the performance analysis is presented in [11,12] for MIMO systems with maximal-ratio transmission, in [13,14] for MIMO systems with STBC. All these performance studies are under the assumption of the perfect channel state information (CSI). For imperfect CSI, system performances were investigated in [15,16] for single transmit antenna selection, where the advantage of combining TAS with STBC is not yet considered. The performance of multi-input and single-output (MISO) system with TAS-STBC in the presence of estimation error and feedback delay over Nakagami-m channels is studied in [17]. The diversity gain obtained in [17] is based on a loose upper bound of the conditional cumulative distribution function, which leads to diversity order of one no matter how many transmit antennas are selected, even when it only considers the presence of feedback delay. Note that this paper is only focused on transmit antenna selection but not on receive antenna selection or path diversity selection [4,19,20]. Compared to the traditional co-located antenna systems, distributed antenna system (DAS) has become a very promising system for future mobile communications [21,22]. The performance between DAS and microcellular systems is compared in [21], and the approach of antenna unit selection in the DAS is presented. In [22], the main advantages and challenges for the DAS-based broadband wireless communications for high speed trains have been discussed and outlined.

In this paper, we study the performance of MIMO-TAS-STBC system with imperfect CSI caused by the feedback delay, when an arbitrary number of antennas are selected, where downlink Rayleigh fading channel is considered. The main contributions of this paper are summarized as follows:

(1) A unified performance analysis of the MIMO-TAS-STBC system with arbitrary number antenna selection is given for imperfect CSI. By theoretical analysis and mathematical manipulation, the moment generating function (MGF) of effective SNR as well as its upper and lower bounds are derived. With these results, we derive the BER of the system with MQAM and MPSK. As a result, accurate and approximate closed-form expressions of BER are obtained. The approximate BER expressions are simpler and give the BER curves close to those of the accurate ones. These expressions include the ones under perfect CSI as special cases. Moreover, simulation results verify the effectiveness of the theoretical analysis.

(2) The diversity gain and coding gain of the system under perfect and imperfect CSI are analyzed. Based on the approximate BER formulae, the upper bounds and lower bounds of BER are derived. Interestingly, these two bounds exhibit the same behavior. With these BER bounds, the diversity gain and coding gain are effectively analyzed. The analysis shows that for imperfect CSI, only partial diversity order is obtained, which is equal to the product of the selective transmit antenna number and receive antenna number. Moreover, the diversity order is not changed as long as the feedback delay exists no matter how small it is. For MISO system under imperfect CSI, the diversity order is then the selective transmit antenna number, while in this case it is only 1 in [17]. Clearly our result is much stronger than that in [17] when Rayleigh fading and only feedback delay are considered. Besides, the antenna numbers, channel correlation coefficients, modulation pattern and rate of STBC will affect the coding gain under imperfect CSI.

(3) The adaptive transmit antenna selection (AAS) scheme is developed for imperfect CSI. Using the simple approximate BER formula, the BERs under different antenna selection cases can be easily calculated. By comparing these BER values, we can easily determine the optimal antenna selection number which has the smallest BER. This optimal antenna selection number may adapt to the change of CSI. Thus, the superior performance will be obtained.

Throughout the paper, the superscripts, bold upper case and lower case letters denote matrices and column vectors, respectively. $E\{\cdot\}$ denotes statistical expectation, and $||\cdot||_F$ is the Frobenius norm.

2 MIMO system model and analysis of effective signal-to-noise ratios

In this paper, we consider a wireless MIMO system with M transmit and N receive antennas operating over a flat and quasi-static Rayleigh fading channel represented by an $N \times M$ fading channel matrix

$\boldsymbol{H} = \{h_{nm}\}$. The complex element h_{nm} denotes the channel gain from the m-th transmit antenna to the n-th receive antenna, which is assumed to be constant over a space-time block coding frame and varies from one frame to another. The channel gains are modeled as independent complex Gaussian random variables (r.v.s) with zero-mean and variance of 0.5 per dimension.

Let $s_m = \sum_{n=1}^{N} |h_{nm}|^2$ for $m = 1, 2, \ldots, M$ denote the instantaneous channel power gain between the m-th transmit antenna and all the receive antennas. For the analysis convenience, the power gains $\{s_m\}$ are sorted in a descending order and denoted by $\{\gamma_m\}$ such that $\gamma_1 \geqslant \gamma_2 \geqslant \cdots \geqslant \gamma_M$. Without loss of generality, it is assumed that K ($K \leqslant M$) best transmit antennas corresponding to $\{\gamma_1, \gamma_2, \ldots, \gamma_K\}$ are chosen for STBC (here high-rate complex orthogonal STBCs in [23] are used for achieving high transmission rate). By utilizing the complex orthogonality of STBC, the received SNR per symbol after the space-time block decoding is expressed as [24]

$$\rho = \frac{P_t}{rK\sigma_n^2} \sum_{k=1}^{K} \gamma_k = \frac{\bar{\rho}}{rK} ||\boldsymbol{H}'||_F^2 = \bar{\rho}' ||\boldsymbol{H}'||_F^2, \tag{1}$$

where $\bar{\rho}' = \bar{\rho}/(rK)$, r is the code rate of an OSTBC, P_t is the total transmit power, σ_n^2 is the noise variance, and $\bar{\rho} = P_t/\sigma_n^2$ is the average SNR per receive antenna, $\boldsymbol{H}'$ is the sub-matrix composed of K columns $\{\boldsymbol{h}'_k, k = 1, 2, \ldots, K\}$ of channel matrix $\boldsymbol{H}$ with$||\boldsymbol{h}'_k||_F^2 = \gamma_k$, and thus $||\boldsymbol{H}'||_F^2 = \sum_{k=1}^{K} \gamma_k$.

Let $\rho_k = \gamma_k \bar{\rho}'$, then the effective SNR $\rho = \rho_1 + \cdots + \rho_K$. According to the analysis above, ρ_k will be a central χ^2 distributed random variable with $2N$ degrees of freedom. From [25, Eq. (2.3-21)], the probability density function (PDF) and corresponding cumulative distribution function (CDF) of ρ_k are, respectively, given

$$f_{\rho_k}(x) = (rKx/\bar{\rho})^N \mathrm{e}^{-xrK/\bar{\rho}}/[x\Gamma(N)] = (x/\bar{\rho}')^N \mathrm{e}^{-x/\bar{\rho}'}/[x\Gamma(N)] \tag{2}$$

and

$$F_{\rho_k}(x) = 1 - \mathrm{e}^{-x/\bar{\rho}'} \sum_{n=0}^{N-1} (x/\bar{\rho}')^n/n!. \tag{3}$$

Using the order statistic [26], the joint PDF of the K selected SNR $\{\rho_1, \ldots, \rho_K\}$ can be given by

$$f_{\rho_1,\ldots,\rho_K}(x_1, \ldots, x_K) = K! \begin{pmatrix} M \\ K \end{pmatrix} [F_{\rho_K}(x_K)]^{M-K} \prod_{k=1}^{K} f_{\rho_k}(x_k). \tag{4}$$

We assume that the channels are perfectly known at the receiver, and the feedback channel is error free, but there is delay in the channel estimation information feedback from the receiver to the transmitter. The transmitter will use the delayed CSI to perform antenna selection. The corresponding delayed SNR, denoted as $\hat{\rho}$, is expressed as

$$\hat{\rho} = \sum_{k=1}^{K} \hat{\rho}_k = \sum_{k=1}^{K} \hat{\gamma}_k \bar{\rho}/(rK) = ||\hat{\boldsymbol{H}}'||_F^2 \bar{\rho}', \tag{5}$$

where $\hat{\boldsymbol{H}}'$ is the τ time-delayed version of $\boldsymbol{H}'$ having the same Gaussian distribution as that of $\boldsymbol{H}'$. The correlation coefficient between the entry $\hat{h}'_{nk}$ of $\hat{\boldsymbol{H}}'$ and h'_{nk} of $\boldsymbol{H}'$ is $c = J_0(2\pi f_d \tau)$, where $J_0(\cdot)$ is the zero-order Bessel function of the first kind [25], τ and f_d are feedback delay and maximum Doppler frequency, respectively. The relationship between the actual channel $\boldsymbol{H}'$ and its delayed version $\hat{\boldsymbol{H}}'$ can be expressed as [27,28]

$$\boldsymbol{H}' = c\hat{\boldsymbol{H}}' + \mathbf{E}, \tag{6}$$

where $\boldsymbol{E}$ is the channel error matrix independent of $\hat{\boldsymbol{H}}'$, whose entries are independently and identically distributed (i.i.d.) complex Gaussian r.v.s with zero mean and variance $\sigma^2 = 1 - c^2$.

Based on the above channel model, using the selected maximum K order statistic, the MGF of $\hat{\rho}$ can be expressed as

$$\Psi_{\hat{\rho}}(s) = \int_0^{\infty} \mathrm{e}^{-sx_1} \int_0^{x_1} \mathrm{e}^{-sx_2} \cdots \int_0^{x_{K-1}} \mathrm{e}^{-sx_K} f_{\hat{\rho}_1,\ldots,\hat{\rho}_K}(x_1, \ldots, x_K) \mathrm{d}x_K \cdots \mathrm{d}x_2 \mathrm{d}x_1. \tag{7}$$

Using [19, (19)], the above Eq. (7) can be written in the following closed-form. i.e.,

$$\Psi_{\hat{\rho}}(s)=\frac{M![\Gamma(N)]^{-K}}{(M-K)!\Gamma(K)}\sum_{l_1,\ldots,l_K}w(N;l_1,\ldots,l_K)\prod_{k=1}^{K-1}\frac{l_k!}{k^{l_k}}\sum_{m=0}^{M-K}\binom{M-K}{m}(-1)^m \times\sum_{n\in\Omega}\binom{m}{n_0,\ldots,n_{N-1}}\frac{(\alpha_{nm}+l_K)!}{\beta_{nm}(1+\bar{\rho}'s)^{d+K-1}}\frac{1}{(K+m+K\bar{\rho}'s)^{\alpha_{nm}+l_K+1}},\tag{8}$$

where $w(N;l_1,\ldots,l_K)$ is the coefficient of $y_1^{l_1}\cdots y_K^{l_K}$ in expression $(\sum_{k=1}^{K}y_k)^{N-1}(\sum_{k=2}^{K}y_k)^{N-1}\cdots y_K^{N-1}$, $d=\sum_{k=1}^{K-1}l_k$, $\binom{m}{n_0,\ldots,n_{N-1}}=\frac{m!}{n_0!\cdots n_{N-1}!}$, $\alpha_{nm}=\sum_{i=1}^{N-1}in_i$, $\beta_{nm}=\prod_{i=1}^{N-1}(i!)^{n_i}$, and Ω is the set of all possible nonnegative-integer combinations of $n_0,\ldots,n_{N-1}$ such that $\sum_{i=0}^{N-1}n_i=m$.

Based on the mathematic derivation in Appendix A, the upper bound and lower bound of MGF, $\Psi_{\hat{\rho}}(s)$, can be, respectively, obtained as

$$\Psi_{\hat{\rho}}^{(u)}(s)=\Gamma(NM+1)_2F_1(1,NM,NM-N+1,0.5)/[2^{NM}(N!)^M(1+s\bar{\rho}')^{NM}],\tag{9}$$

and

$$\Psi_{\hat{\rho}}^{(l)}(s)=\frac{\Gamma(NM+1)}{(N!)^M(M+K\bar{\rho}'s)^{NM}}{}_2F_1\left(1,NM,NM-N+1,\frac{(K-1)\bar{\rho}'s+M-1}{K\bar{\rho}'s+M}\right),\tag{10}$$

where ${}_2F_1(x,y;w;z)$ is the Gaussian hypergeometric function [29].

Compared to the accurate MGF in (8), (9) and (10) have simpler forms. Moreover, they will help us to perform the asymptotical performance analysis and achieve the diversity gain and coding gain.

By means of partial fraction decomposition, Eq. (8) can be rewritten as

$$\Psi_{\hat{\rho}}(s)=\binom{M}{K}\sum_{l_1,\ldots,l_K}\frac{w(N;l_1,\ldots,l_K)}{[\Gamma(N)]^K}\prod_{k=1}^{K-1}\frac{l_k!}{k^{l_k}}\left\{\frac{l_K!K^{-l_K}}{(1+s\bar{\rho}')^{NK}}+\sum_{m=1}^{M-K}\binom{M-K}{m}(-1)^m \times\sum_{n\in\Omega}\binom{m}{n_0,\ldots,n_{N-1}}\frac{(\alpha_{nm}+l_K)!K^{d+K}}{\beta_{nm}m^{NK+\alpha_{nm}}}\left[\sum_{j=1}^{d+K-1}\frac{A_j}{(s+\bar{\rho}'^{-1})^j}+\sum_{j=1}^{\alpha_{nm}+l_K+1}\frac{B_j}{(s+(K+m)/(K\bar{\rho}'))^j}\right]\right\},\tag{11}$$

where $A_j=\binom{NK+\alpha_{nm}-j-1}{\alpha_{nm}+l_K}\frac{(-1)^{d+K-j-1}}{(K\bar{\rho}'/m)^j}$, and $B_j=\binom{NK+\alpha_{nm}-j-1}{d+K-2}\frac{(-1)^{d+K-1}}{(K\bar{\rho}'/m)^j}$.

With (11), using the inverse Laplace transform, closed-form PDF of $\hat{\rho}$ can be attained as

$$f_{\hat{\rho}}(y)=\binom{M}{K}\sum_{l_1,\ldots,l_K}\frac{w(N;l_1,\ldots,l_K)}{[\Gamma(N)]^K}\prod_{k=1}^{K-1}\frac{l_k!}{k^{l_k}}\left\{\frac{l_K!y^{NK-1}\mathrm{e}^{-y/\bar{\rho}'}}{K^{l_K}\bar{\rho}'^{NK}\Gamma(NK)}+\sum_{m=1}^{M-K}\binom{M-K}{m}(-1)^m \times\sum_{n\in\Omega}\binom{m}{n_0,\ldots,n_{N-1}}\frac{(\alpha_{nm}+l_K)!K^{d+K}}{\beta_{nm}m^{NK+\alpha_{nm}}}\left[\sum_{j=1}^{d+K-1}A_j\frac{y^{j-1}}{\Gamma(j)}\mathrm{e}^{-\frac{y}{\bar{\rho}'}}+\sum_{j=1}^{\alpha_{nm}+l_K+1}B_j\frac{y^{j-1}}{\Gamma(j)}\mathrm{e}^{-\frac{K+m}{K\bar{\rho}'}y}\right]\right\}.\tag{12}$$

This is also a closed-form PDF expression of the SNR in (1) under perfect CSI. Although [18] gives the PDF expression of the SNR under perfect CSI, the obtained PDF is not always valid (see [18, (7)]). This is because it cannot be used for the calculation when the index in the summation term $j=0$. Besides, the closed-form expressions of the coefficients for inverse Laplace transform (i.e., P_m and Q_l in [18, (7)]) are also not provided.

According to the channel model (6), conditioned on $\hat{\boldsymbol{H}}'$, the elements $\{h'_{nk}\}$ of $\boldsymbol{H}'$ are complex Gaussian distributed with mean $c\hat{h}'_{nk}$ and variance $\sigma^2 = 1 - c^2$. With these independent Gaussian distributed $\{h'_{nk}\}$, $\lambda = ||\boldsymbol{H}'||_F^2$ will become independent noncentral chi-square distributed. Utilizing in [25, Eq. (2.1-118)], the PDF of λ conditioned on $\hat{\boldsymbol{H}}'$ can be expressed by

$$f(\lambda|\hat{\boldsymbol{H}}') = \frac{1}{\sigma^2}\left(\frac{\lambda}{c^2\hat{\lambda}}\right)^{(NK-1)/2} I_{NK-1}\left(\sqrt{\lambda\hat{\lambda}}\frac{2c}{\sigma^2}\right)\exp\left(-\frac{\lambda + c^2\hat{\lambda}}{\sigma^2}\right), \tag{13}$$

where $\hat{\lambda} = ||\hat{\boldsymbol{H}}'||_F^2$, and $I_a(\cdot)$ is the ath-order modified Bessel function of the first kind. According to (5) and using the transformation of variable, the conditional PDF of the received SNR $\rho = \lambda\bar{\rho}'$, given the estimate $\hat{\rho}$, can be expressed as [30]

$$f_{\rho|\hat{\rho}}(x|y) = \frac{1}{\sigma^2\bar{\rho}'}\left(\frac{x}{c^2y}\right)^{(NK-1)/2} I_{NK-1}\left(\sqrt{xy}\frac{2c}{\bar{\rho}'\sigma^2}\right)\exp\left(-\frac{x + c^2y}{\bar{\rho}'\sigma^2}\right). \tag{14}$$

With (12) and (14), the MGF of received SNR ρ, $\Psi_\rho(s)$, is given by

$$\begin{aligned}\Psi_\rho(s) &= E\{\mathrm{e}^{-s\rho}\}\\ &= \int_0^\infty\int_0^\infty \frac{1}{\sigma^2\bar{\rho}'}\left(\frac{x}{c^2y}\right)^{(NK-1)/2} I_{NK-1}\left(\sqrt{xy}\frac{2c}{\bar{\rho}'\sigma^2}\right)\exp\left(-\frac{x + c^2y}{\bar{\rho}'\sigma^2} - sx\right)\mathrm{d}x f_{\hat{\rho}}(y)\mathrm{d}y.\end{aligned} \tag{15}$$

Utilizing the equation $\int_0^\infty x^{m/2}\mathrm{e}^{-\alpha x}I_m(2\beta\sqrt{x})\mathrm{d}x = (\beta^m/\alpha^{m+1})\mathrm{e}^{\beta^2/\alpha}$ [29], Eq. (15) can be expressed as

$$\Psi_\rho(s) = \frac{1}{(1 + \sigma^2\bar{\rho}'s)^{NK}}\Psi_{\hat{\rho}}\left(\frac{c^2s}{1 + \sigma^2\bar{\rho}'s}\right). \tag{16}$$

Substituting (8) into (16) yields

$$\begin{aligned}\Psi_\rho(s) = {}& \frac{M![\Gamma(N)]^{-K}}{(M-K)!\Gamma(K)}\sum_{l_1,\ldots,l_K} w(N; l_1, \ldots, l_K)\prod_{k=1}^{K-1}\frac{l_k!}{k^{l_k}}\sum_{m=0}^{M-K}\binom{M-K}{m}(-1)^m\\ &\times\sum_{n\in\Omega}\binom{m}{n_0,\ldots,n_{N-1}}\frac{(\alpha_{nm}+l_K)!}{\beta_{nm}(1+\bar{\rho}'s)^{d+K-1}}\frac{(1+\sigma^2\bar{\rho}'s)^{\alpha_{nm}}}{(K+m+m\sigma^2\bar{\rho}'s+K\bar{\rho}'s)^{\alpha_{nm}+l_K+1}}.\end{aligned} \tag{17}$$

Substituting (11) into (16) yields another expression of MGF, i.e.,

$$\begin{aligned}\Psi_\rho(s) = {}& \binom{M}{K}\sum_{l_1,\ldots,l_K}\frac{w(N; l_1, \ldots, l_K)}{[\Gamma(N)]^K}\prod_{k=1}^{K-1}\frac{l_k!}{k^{l_k}}\left\{\frac{l_K!K^{-l_K}}{(1+s\bar{\rho}')^{NK}} + \sum_{m=1}^{M-K}\binom{M-K}{m}\right.\\ &\times\sum_{n\in\Omega}\binom{m}{n_0,\ldots,n_{N-1}}(-1)^m\frac{(\alpha_{nm}+l_K)!K^{d+K}}{\beta_{nm}m^{NK+\alpha_{nm}}}\left[\sum_{j=1}^{d+K-1}\frac{A_j(1+\sigma^2\bar{\rho}'s)^{j-NK}}{(s+\bar{\rho}'^{-1})^j}\right.\\ &\left.\left.+\sum_{j=1}^{\alpha_{nm}+l_K+1}\frac{B_j(1+\sigma^2\bar{\rho}'s)^{j-NK}}{(s+(K+m+m\sigma^2\bar{\rho}'s)/(K\bar{\rho}'))^j}\right]\right\}.\end{aligned} \tag{18}$$

Eqs. (17) and (18) are closed-form MGF of the effective SNR ρ of MIMO with TAS and STBC in the presence of imperfect CSI. When the CSI is perfectly known, $c^2 = 1$, Eqs. (17) and (18) are reduced to the MGF under perfect CSI given as (8) and (11), respectively. Besides, substituting (9) and (10) into (16), we can obtain an upper bound and lower bound of MGF of effective SNR, respectively.

3 Performance analysis

In this section, we will analyze the performance of MIMO-TAS-STBC system under imperfect CSI, and give the derivation of BER of the system so that the system performance can be evaluated in theory.

3.1 Accurate BER analysis

According to [31], the BER of MQAM with Gray mapping over AWGN is given by

$$P_{e,\mathrm{q}}(\rho)=\sum_{v=1}^{N_Q}\xi_v\mathrm{erfc}(\sqrt{\eta_{\mathrm{v}}\rho})=\frac{2}{\pi}\sum_{v=1}^{\mathrm{N_Q}}\xi_{\mathrm{v}}\int_0^{\pi/2}\exp\Big(-\frac{\eta_{\mathrm{v}}\rho}{\sin^2\theta}\Big)\mathrm{d}\theta, \tag{19}$$

where $\mathrm{erfc}(z)=(2/\sqrt{\pi})\int_z^{\infty}\exp(-x^2)\mathrm{d}x$ is the complementary error function [29], ξ_v and η_v are constants which depend on the constellation size Q, and the values $\{\xi_v,\eta_v\}$ for MQAM can be found in [31], N_Q is the number of terms for summation, and q in the subscript of $P_{e,\mathrm{q}}$ stands for QAM constellation. Hence, using (18) and (19), the BER of MIMO-TAS-STBC with MQAM under imperfect CSI is expressed as

$$\hat{P}_{e,\mathrm{q}}=\frac{2}{\pi}\sum_{v=1}^{N_Q}\xi_v\int_0^{\infty}\int_0^{\pi/2}\exp\Big(-\frac{\eta_v x}{\sin^2\theta}\Big)f_\rho(x)\mathrm{d}\theta\mathrm{d}x=\frac{2}{\pi}\sum_{v=1}^{N_Q}\xi_v\int_0^{\pi/2}\Psi_\rho\Big(\frac{\eta_v}{\sin^2\theta}\Big)\mathrm{d}\theta. \tag{20}$$

Utilizing the equality

$$\frac{2}{\pi}\int_0^{\pi/2}(1+c\sin^{-2}\theta)^{-k}\mathrm{d}\theta=1-\mu\sum_{i=0}^{k-1}\binom{2i}{i}\Big(\frac{1-\mu^2}{4}\Big)^i,$$

and $\mu=\sqrt{\frac{c}{c+1}}$ [32], by means of the mathematical derivation, Eq. (20) can be given by

$$\begin{aligned}\hat{P}_{e,\mathrm{q}}=&\sum_{v=1}^{N_Q}\xi_v\binom{M}{K}\sum_{l_1,\ldots,l_K}\frac{w(N;l_1,\ldots,l_K)}{[\Gamma(N)]^K}\prod_{k=1}^{K-1}\frac{l_k!}{k^{l_k}}\Bigg\{\frac{l_K!}{K^{l_K}}\Big(1-\mu_{q1}\sum_{i=0}^{NK-1}\binom{2i}{i}\Big(\frac{1-\mu_{q1}^2}{4})^i\Big)\\&+\sum_{m=1}^{M-K}(-1)^m\times\binom{M-K}{m}\sum_{n\in\Omega}\binom{m}{n_0,\ldots,n_{N-1}}\frac{(\alpha_{nm}+l_K)!K^{d+K}}{\beta_{nm}m^{NK+\alpha_{nm}}}\Bigg[\sum_{j=1}^{d+K-1}A_j\bar{\rho}'^jI_{1,q}\\&+\sum_{z=1}^{\alpha_{nm}+l_K+1}\frac{B_z(K\bar{\rho}')^z}{(K+m\sigma^2)^{z-NK}}I_{2,q}\Bigg]\Bigg\},\end{aligned} \tag{21}$$

where the details on derivation are omitted due to the space limitation, $I_{1,q}$ and $I_{2,q}$ can be calculated with the following closed-forms,

$$\begin{aligned}I_{1,q}=&\sum_{u=1}^{j}\binom{NK-u-1}{NK-j-1}\frac{(-\sigma^2)^{j-u}}{c^{2(NK-u)}}\Big(1-\mu_{q1}\sum_{i=0}^{u-1}\binom{2i}{i}\Big(\frac{1-\mu_{q1}^2}{4}\Big)^i\Big)\\&+\sum_{v=1}^{NK-j}\binom{NK-v-1}{j-1}\frac{(-\sigma^2)^j}{c^{2(NK-v)}}\Big(1-\mu_{q3}\sum_{i=0}^{v-1}\binom{2i}{i}\Big(\frac{1-\mu_{q3}^2}{4}\Big)^i\Big)\end{aligned} \tag{22}$$

and

$$\begin{aligned}I_{2,q}=&\sum_{s=1}^{z}\binom{NK-s-1}{NK-z-1}\frac{(-\sigma^2)^{z-s}(K+m)^{-s}}{(Kc^2)^{NK-s}}\Big(1-\mu_{q2}\sum_{i=0}^{s-1}\binom{2i}{i}\Big(\frac{1-\mu_{q2}^2}{4}\Big)^i\Big)\\&+\sum_{t=1}^{NK-z}\binom{NK-t-1}{j-1}\frac{(-\sigma^2)^z(Kc^2)^{t-NK}}{(K+m\sigma^2)^{t+z-NK}}\Big(1-\mu_{q3}\sum_{i=0}^{t-1}\binom{2i}{i}\Big(\frac{1-\mu_{q3}^2}{4}\Big)^i\Big),\end{aligned} \tag{23}$$

where $\mu_{q1}=\sqrt{\frac{\eta_v\bar{\rho}'}{\eta_v\bar{\rho}'+1}}$, $\mu_{q2}=\sqrt{\frac{\eta_v\bar{\rho}'(m\sigma^2+K)}{\eta_v\bar{\rho}'(m\sigma^2+K)+m+K}}$ and $\mu_{q3}=\sqrt{\frac{\eta_v\bar{\rho}'\sigma^2}{\eta_v\bar{\rho}'\sigma^2+1}}$. Eq. (21) is a closed-form expression of BER of MIMO-TAS-STBC with MQAM under imperfect CSI. This expression does not need any integration and can be easily calculated with high accuracy. It is shown that Eq. (21) is accurate by computer simulation.

For perfect feedback, $c^2=1$, Eq. (21) will be reduced to

$$P_{e,\mathrm{q}}=\binom{M}{K}\sum_{v=1}^{N_Q}\frac{\xi_v}{[\Gamma(N)]^K}\sum_{l_1,\ldots,l_K}w(N;l_1,\ldots,l_K)\prod_{k=1}^{K-1}\frac{l_k!}{k^{l_k}}\Bigg\{\frac{l_K!}{K^{l_K}}\Bigg(1-\mu_{q1}\sum_{i=0}^{NK-1}\binom{2i}{i}\Big(\frac{1-\mu_{q1}^2}{4}\Big)^i\Bigg)$$
$$+\sum_{m=1}^{M-K}\binom{M-K}{m}(-1)^m\sum_{n\in\Omega}\binom{m}{n_0,\ldots,n_{N-1}}\frac{(\alpha_{nm}+l_K)!K^{d+K}}{\beta_{nm}m^{NK+\alpha_{nm}}}$$
$$\times\Bigg[\sum_{j=1}^{d+K-1}A_j\bar{\rho}'^j\Bigg(1-\mu_{q1}\sum_{i=0}^{j-1}\binom{2i}{i}\Big(\frac{1-\mu_{q1}^2}{4}\Big)^i\Bigg)$$
$$+\sum_{u=1}^{\alpha_{nm}+l_K+1}B_u\Big(\frac{\bar{\rho}'K}{m+K}\Big)^u\Bigg(1-\mu_{q2}\sum_{i=0}^{u-1}\binom{2i}{i}\Big(\frac{1-\mu_{q2}^2}{4}\Big)^i\Bigg)\Bigg]\Bigg\},\tag{24}$$

where $\mu_{q1}=\sqrt{\eta_v\bar{\rho}'/(\eta_v\bar{\rho}'+1)}$, $\mu_{q2}=\sqrt{\eta_v\bar{\rho}'K/(\eta_v\bar{\rho}'K+m+K)}$. Eq. (24) is a closed-form expression of BER of MIMO-TAS-STBC with MQAM under perfect CSI, and this theoretical expression is shown to match the simulation well. Although the accurate BER expression is also provided in [13] for perfect CSI, the expression needs to compute the integral by using the residue theorem. Thus, it is not completely a closed-form and has relatively high complexity.

Utilizing [33, Eq. (12)] and (18), the BER of MIMO-TAS-STBC with MPSK and Gray mapping can be expressed as

$$\hat{P}_{e,\mathrm{p}}\cong\binom{M}{K}\sum_{v=1}^{\max(Q/4,1)}\sum_{l_1,\ldots,l_K}\frac{w(N;l_1,\ldots,l_K)}{\max(q,2)[\Gamma(N)]^K}\prod_{k=1}^{K-1}\frac{l_k!}{k^{l_k}}\Bigg\{\frac{l_K!}{K^{l_K}}\Bigg(1-\mu_{p1}\sum_{i=0}^{NK-1}\binom{2i}{i}\Big(\frac{1-\mu_{p1}^2}{4}\Big)^i\Bigg)$$
$$+\sum_{m=1}^{M-K}\binom{M-K}{m}(-1)^m\sum_{n\in\Omega}\binom{m}{n_0,\ldots,n_{N-1}}\frac{(\alpha_{nm}+l_K)!K^{d+K}}{\beta_{nm}m^{NK+\alpha_{nm}}}\Bigg[\sum_{j=1}^{d+K-1}A_j\bar{\rho}'^jI_{1,p}$$
$$+\sum_{z=1}^{\alpha_{nm}+l_K+1}\frac{B_z(K\bar{\rho}')^z}{(K+m\sigma^2)^{z-NK}}I_{2,p}\Bigg]\Bigg\},\tag{25}$$

where the subscript p stands for PSK constellation, $q=\log_2 Q$, $g_v=\sin^2(\pi(2v-1)/Q)$, $I_{1,p}$ can be obtained by replacing $\mu_{q,1}$ with $\mu_{p,1}$ and $\mu_{q,3}$ with $\mu_{p,3}$ in (22), and $I_{2,p}$ can be attained by replacing $\mu_{q,2}$ with $\mu_{p,2}$ and $\mu_{q,3}$ with $\mu_{p,3}$ in (23), where $\mu_{p1}=\sqrt{g_v\bar{\rho}'/(g_v\bar{\rho}'+1)}$, $\mu_{p3}=\sqrt{g_v\bar{\rho}'\sigma^2/(g_v\bar{\rho}'\sigma^2+1)}$, and $\mu_{p2}=\sqrt{g_v\bar{\rho}'(m\sigma^2+K)/[g_v\bar{\rho}'(m\sigma^2+K)+m+K]}$. This is a tight closed-form expression of BER of MIMO-TAS-STBC with MPSK in the presence of imperfect CSI. This expression is shown to be very close to simulation results. It is well-known that the BERs of BPSK and QPSK over AWGN [31] are $P_{e,p}(\rho)=0.5\mathrm{erfc}(\sqrt{\rho})$ and $P_{e,p}(\rho)=0.5\mathrm{erfc}(\sqrt{\rho/2})$. So Eq. (25) is also an accurate closed-form expression of BER of MIMO-TAS-STBC with BPSK and QPSK.

With perfect CSI, $c^2=1$, Eq. (25) will be reduced to

$$P_{e,\mathrm{p}}\cong\binom{M}{K}\sum_{v=1}^{\max(Q/4,1)}\sum_{l_1,\ldots,l_K}\frac{w(N;l_1,\ldots,l_K)}{[\Gamma(N)]^K\max(q,2)}\prod_{k=1}^{K-1}\frac{l_k!}{k^{l_k}}\Bigg\{\frac{l_K!}{K^{l_K}}\Bigg(1-\mu_{p1}\sum_{i=0}^{NK-1}\binom{2i}{i}\Big(\frac{1-\mu_{p1}^2}{4}\Big)^i\Bigg)$$
$$+\sum_{m=1}^{M-K}\binom{M-K}{m}(-1)^m\sum_{n\in\Omega}\binom{m}{n_0,\ldots,n_{N-1}}\frac{(\alpha_{nm}+l_K)!K^{d+K}}{\beta_{nm}m^{NK+\alpha_{nm}}}$$
$$\times\Bigg[\sum_{j=1}^{d+K-1}A_j\bar{\rho}'^j\Bigg(1-\mu_{p1}\sum_{i=0}^{j-1}\binom{2i}{i}\Big(\frac{1-\mu_{p1}^2}{4}\Big)^i\Bigg)$$
$$+\sum_{u=1}^{\alpha_{nm}+l_K+1}B_u\Big(\frac{\bar{\rho}'K}{m+K}\Big)^u\Bigg(1-\mu_{p2}\sum_{i=0}^{u-1}\binom{2i}{i}\Big(\frac{1-\mu_{p2}^2}{4}\Big)^i\Bigg)\Bigg]\Bigg\},\tag{26}$$

where $\mu_{p1}=\sqrt{g_v\bar{\rho}'/(g_v\bar{\rho}'+1)}$, $\mu_{p2}=\sqrt{g_v\bar{\rho}'K/(g_v\bar{\rho}'K+m+K)}$. Eq. (26) is a tight closed-form expression of BER of MIMO-TAS-STBC with MPSK under perfect CSI.

3.2 Approximate BER analysis

In this subsection, to simplify the calculation of BERs, simple approximate BER expressions of the MIMO-TAS-STBC system with imperfect CSI will be derived.

According to [34], the complementary error function $\mathrm{erfc}(x)$ can be accurately approximated as

$$\mathrm{erfc}(t) \cong a_1 \exp(-b_1 t^2) + a_2 \exp(-b_2 t^2), \qquad t > 0, \tag{27}$$

where $a_1 = 0.416, b_1 = 1.942; a_2 = 0.294, b_2 = 1.05$.

Substituting (27) into (19) yields

$$P_{e,\mathrm{q}}(\rho) \cong \sum_{v=1}^{N_Q} \xi_v \sum_{i=1}^{2} a_i \exp(-b_i \eta_v \rho). \tag{28}$$

Using (20) and (16), the BER of MIMO-TAS-STBC with MQAM under imperfect CSI can be expressed as

$$\hat{P}_{e,\mathrm{q}} \cong \sum_{i=1}^{2} \sum_{v=1}^{N_Q} \xi_v a_i \Psi_\rho(b_i \eta_v) = \sum_{i=1}^{2} \sum_{v=1}^{N_Q} \frac{\xi_v a_i}{(1+\sigma^2 \bar{\rho}' b_i \eta_v)^{NK}} \Psi_{\hat{\rho}}\left(\frac{c^2 b_i \eta_v}{1+\sigma^2 \bar{\rho}' b_i \eta_v}\right). \tag{29}$$

Substituting (8) into (29) gives

$$\begin{aligned} \hat{P}_{e,\mathrm{q}} \cong & \binom{M}{K} \sum_{i=1}^{2} \sum_{v=1}^{N_Q} \frac{K \xi_v a_i}{[\Gamma(N)]^K} \sum_{l_1,\ldots,l_K} w(N; l_1, \ldots, l_K) \prod_{k=1}^{K-1} \frac{l_k!}{k^{l_k}} \sum_{m=0}^{M-K} \binom{M-K}{m} (-1)^m \\ & \times \sum_{n \in \Omega} \binom{m}{n_0, \ldots, n_{N-1}} \frac{(\alpha_{nm} + l_K)! (1+\sigma^2 \bar{\rho}' b_i \eta_v)^{\alpha_{nm}}}{\beta_{nm} (1+\bar{\rho}' b_i \eta_v)^{d+K-1} [K + m + (m\sigma^2 + K) \bar{\rho}' b_i \eta_v]^{\alpha_{nm} + l_K + 1}}. \end{aligned} \tag{30}$$

Eq. (30) is an approximate closed-form expression of BER of MIMO-TAS-STBC with MQAM in the presence of imperfect CSI. Compared with the accurate BER derived in Subsection 3.1, the obtained approximate BER has much fewer terms in the summation. Moreover, the accurate BER needs to compute the coefficients for inverse Laplace transform by using partial fractions and inverse Laplace transform, while the approximate BER does not need these computations. Thus, the approximate BER has relatively lower complexity. Besides, due to better approximation, it will have the value close to the accurate one.

Similarly, we can derive the approximate closed-form expressions of BER of MIMO-TAS-STBC with MPSK for imperfect CSI as follows:

$$\begin{aligned} \hat{P}_{e,\mathrm{p}} \cong & \binom{M}{K} \frac{[\Gamma(N)]^{-K} K}{\max(q,2)} \sum_{i=1}^{2} \sum_{v=1}^{\max(Q/4,1)} \sum_{l_1,\ldots,l_K} w(N; l_1, \ldots, l_K) \prod_{k=1}^{K-1} \frac{l_k!}{k^{l_k}} \sum_{m=0}^{M-K} \binom{M-K}{m} \\ & \times (-1)^m \sum_{n \in \Omega} \binom{m}{n_0, \ldots, n_{N-1}} \frac{a_i (\alpha_{nm} + l_K)! (1+\sigma^2 \bar{\rho}' b_i g_v)^{\alpha_{nm}}}{\beta_{nm} (1+\bar{\rho}' b_i g_v)^{d+K-1} [K + m + (m\sigma^2 + K) \bar{\rho}' b_i g_v]^{\alpha_{nm} + l_K + 1}}. \end{aligned} \tag{31}$$

With the perfect feedback, $c^2 = 1$, Eqs. (30) and (31) are reduced to the approximate closed-form expression of BER of MIMO-TAS-STBC with MQAM and MPSK under perfect CSI, respectively. Besides, our analytical method may also be applicable for the distributed antenna system for the performance evaluation by the extension.

4 Asymptotic performance analysis

In this section, we will give the asymptotic performance analysis of MIMO-TAS-STBC at high SNR and an adaptive antenna selection scheme in terms of feedback CSI.

4.1 Diversity gain and coding gain

Based on the derived approximate BER as well as the lower bound and upper bound of MGF (as shown in (9) and (10)), we will further derive lower and upper bounds of BER at high SNR. With these results, the diversity gain and coding gain of MIMO-TAS-STBC will be obtained. Substituting (9) and (10) into (29), we can obtain the upper bound and lower bound of BER of the system with MQAM as follows:

$$\hat{P}_{\mathrm{e,q}}^{(u)} = \sum_{j=1}^{2}\sum_{v=1}^{N_Q} \xi_v a_j \frac{\Gamma(NM+1)}{(N!)^M} \frac{(1+\sigma^2 b_j \eta_v \bar{\rho}')^{NM-NK}}{(1+b_j\eta_v\bar{\rho}')^{NM} 2^{NM}} {}_2F_1(1, NM, NM-N+1, 0.5) \tag{32}$$

and

$$\begin{aligned}\hat{P}_{\mathrm{e,q}}^{(l)} = &\sum_{j=1}^{2}\sum_{v=1}^{N_Q} \xi_v a_j \frac{\Gamma(NM+1)}{(N!)^M} \frac{(1+\sigma^2 b_j \eta_v \bar{\rho}')^{NM-NK}}{(Kc^2 b_j\eta_v\bar{\rho}' + M\sigma^2 b_j\eta_v\bar{\rho}' + M)^{NM}} \\ &\times {}_2F_1\left(1, NM, NM-N+1, \frac{(K-1)c^2 b_j\eta_v\bar{\rho}' + (M-1)\sigma^2 b_j\eta_v\bar{\rho}' + M - 1}{Kc^2 b_j\eta_v\bar{\rho}' + M\sigma^2 b_j\eta_v\bar{\rho}' + M}\right).\end{aligned} \tag{33}$$

According to the upper and lower bounds of BER in (32) and (33), we can evaluate the diversity gain G_d and coding gain G_c, which are important error performance indicators. G_d and G_c are, respectively, defined as the slope and offset of BER curve for average SNR $\bar{\rho}$ approaching infinity [35] and expressed as

$$G_d = \lim_{\bar{\rho}\to\infty} -\frac{\log(\mathrm{P}_{e,\mathrm{q}})}{\log(\bar{\rho})} \quad \text{and} \quad G_c = \lim_{\bar{\rho}\to\infty} \frac{(\mathrm{P}_{e,\mathrm{q}})^{-1/G_d}}{\bar{\rho}}. \tag{34}$$

For imperfect CSI, c^2 is not equal to 1, and $\sigma^2 = 1 - c^2 \neq 0$. So when the SNR is large, Eqs. (32) and (33) become

$$\hat{P}_{e,\mathrm{q}}^{(u)} \approx \sum_{j=1}^{2}\sum_{v=1}^{N_Q} \xi_v a_j \frac{\Gamma(NM+1)}{(N!)^M} \frac{(\sigma^2)^{NM-NK}(rK)^{NK}}{2^{NM}(b_j\eta_v)^{NK}\bar{\rho}^{NK}} {}_2F_1(1, NM, NM-N+1, 0.5) \tag{35}$$

and

$$\hat{P}_{e,\mathrm{q}}^{(l)} \approx \sum_{j=1}^{2}\sum_{v=1}^{N_Q} \frac{\xi_v a_j \Gamma(NM+1)(\sigma^2)^{NM-NK}(rK)^{NK}}{(N!)^M (Kc^2+M\sigma^2)^{NM}(b_j\eta_v)^{NK}\bar{\rho}^{NK}} {}_2F_1\left(1, NM, NM-N+1, \frac{Kc^2+M\sigma^2-1}{Kc^2+M\sigma^2}\right). \tag{36}$$

Applying the definition of G_d in (34) to (35) and (36), the diversity gain is

$$G_d = \lim_{\bar{\rho}\to\infty} -\frac{\log(\hat{P}_{e,\mathrm{q}}^{(i)})}{\log(\bar{\rho})} = \lim_{\bar{\rho}\to\infty} -\frac{-\log(\bar{\rho}^{NK})}{\log(\bar{\rho})} = NK, \quad i = u, l. \tag{37}$$

Hence, the MIMO-TAS-STBC system can achieve the partial diversity order of NK in the presence of imperfect CSI. It is shown in (37) that the slopes of the upper and lower bound of BER curves are equal to NK. Thus, under imperfect CSI, the more the selective antenna number K, the larger the diversity order is. Based on this, all transmit antennas should be selected for achieving superior performance at high SNR.

According to the definition of G_c in (34), the coding gain of the system under imperfect CSI can be obtained from (35) as

$$G_c = \left[\sum_{j=1}^{2}\sum_{v=1}^{N_Q} \frac{\xi_v a_j \Gamma(NM+1)(1-c^2)^{NM-NK}}{(N!)^M 2^{NM}} {}_2F_1(1, NM, NM-N+1, 0.5)\right]^{-\frac{1}{NK}} \frac{b_j\eta_v}{rK}. \tag{38}$$

From (38), it is found that the transmit antenna number, M, and receive antenna number, N, selective antenna number, K, code rate, r, correlation coefficients, c, and modulation pattern will affect the coding gain of the system under imperfect CSI.

For perfect CSI, $c^2 = 1$, and $\sigma^2 = 1 - c^2 = 0$. Thus, Eqs. (32) and (33) are reduced to

$$P_{e,\mathrm{q}}^{(u)} = \sum_{j=1}^{2}\sum_{v=1}^{N_Q} \xi_v a_j \frac{\Gamma(NM+1)}{(N!)^M} \frac{1}{(1+b_j\eta_v\bar{\rho}')^{NM} 2^{NM}} {}_2F_1(1, NM, NM-N+1, 0.5) \tag{39}$$

and

$$P_{e,\mathrm{q}}^{(l)} = \sum_{j=1}^{2}\sum_{v=1}^{N_Q} \frac{\xi_v a_j \Gamma(NM+1)}{(N!)^M (Kb_j\eta_v\bar{\rho}'+M)^{NM}} {}_2F_1\left(1, NM, NM-N+1, \frac{(K-1)b_j\eta_v\bar{\rho}'+M-1}{Kb_j\eta_v\bar{\rho}'+M}\right). \tag{40}$$

When the SNR is large, Eq. (39) and (40) become

$$P_{e,\mathrm{q}}^{(u)} \approx \sum_{j=1}^{2}\sum_{v=1}^{N_Q} \xi_v a_j \frac{\Gamma(NM+1)}{(N!)^M} \frac{(rK)^{NM}}{(2b_j\eta_v)^{NM}\bar{\rho}^{NM}} {}_2F_1(1, NM, NM-N+1, 0.5) \tag{41}$$

and

$$P_{e,\mathrm{q}}^{(l)} \approx \sum_{j=1}^{2}\sum_{v=1}^{N_Q} \xi_v a_j \frac{\Gamma(NM+1)(rK)^{NM}}{(N!)^M (Kb_j\eta_v)^{NM}\bar{\rho}^{NM}} {}_2F_1\left(1, NM, NM-N+1, \frac{K-1}{K}\right). \tag{42}$$

From the definition of G_d in (34), using (41) and (42), we can evaluate the diversity gain as

$$G_d = \lim_{\bar{\rho}\to\infty} -\frac{\log(\mathrm{P}_{e,\mathrm{q}}^{(i)})}{\log(\bar{\rho})} = \lim_{\bar{\rho}\to\infty} -\frac{-\log(\bar{\rho}^{MN})}{\log(\bar{\rho})} = MN, \quad i = u, l. \tag{43}$$

Thus, the system can obtain the full diversity order of MN under perfect CSI. By the definition of G_c in (34), the coding gain of the system under perfect CSI can be obtained from (41) as

$$G_c = \left[\sum_{j=1}^{2}\sum_{v=1}^{N_Q} \frac{\xi_v a_j \Gamma(NM+1)}{(N!)^M} {}_2F_1(1, NM, NM-N+1, 0.5)\right]^{-\frac{1}{NM}} \frac{2b_j\eta_v}{rK}. \tag{44}$$

From (44), it is found that the transmit antenna number, receive antenna number, selective antenna number, code rate and modulation mode will affect the coding gain under perfect CSI.

Similarly, using the analytical method above, we can obtain the diversity gain and coding gain of MIMO-TAS-STBC with MPSK, that is, full diversity order of MN for perfect CSI and partial diversity order of NK for imperfect CSI. Moreover, their coding gains have the forms similar to those with MQAM except that the modulation parameters are different.

4.2 Selective antenna number K

According to the asymptotic analysis above, the selective antenna number K has a significant influence on the system performance (including diversity gain and coding gain), especially in the presence of imperfect CSI. For this reason, we will give an adaptive antenna selection method in terms of the available CSI so that the superior performance may be obtained.

For perfect CSI, from (44), it is observed that the coding gain will become small with the increase of rK. Considering that the product of r and K is larger than 1 for OSTBC, one antenna selection (K=1) will be the best choice for the coding gain of the system under perfect CSI. This is because r=1 in the case of K=1 (corresponding rK=1). Recall that in the case of perfect CSI, selecting one transmit antenna, i.e., K=1, the full spatial diversity from all the transmit antennas is already achieved [5,6]. As a result, the system performance is the best. Whereas under imperfect CSI, K=1 is no longer optimal, and the optimal K will be different under different SNRs and CSI feedback, which can be seen from (37) and (38). For this, we will propose an adaptive antenna selection scheme for determining K based on the approximate BER. This is because it has simple expression and better approximation. The design procedure is shown as follows:

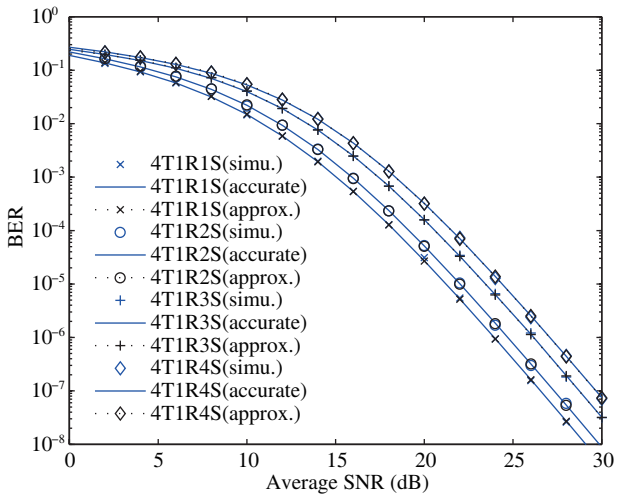

Figure 1 (Color online) BER of MIMO-TAS-STBC with 4 transmit antennas and 1 receive antenna under perfect CSI.

(1) Set the system parameters, such as system configuration (transmit antenna M, receive antenna N), modulation mode, channel correlation coefficient, and average SNR.

(2) Calculate respective approximate BERs by means of (30) or (31) for different $K = 1, 2, \ldots, M$, which are denoted as $\{P_e(K), K = 1, 2, \ldots, M\}$.

(3) Comparing these theoretical $\{P_e(K), K = 1, 2, \ldots, M\}$, we can easily find the minimum value among these $\{P_e(K)\}$, denoted as $\{P_e(K^*)\}$. Thus, the optimal K^* is determined. In other words, using this K^*, the calculated $\{P_e(K)\}$ is the minimum.

(4) Using K^* and (21) or (25), compute the BER, and accurate theoretical BER is obtained.

(5) Employing the above method, the 'best' BER under different average SNRs can be obtained.

According to the above analysis, the optimal selective antenna number K^* can adapt to the changes of CSI. Hence, with the above-mentioned adaptive scheme, we can achieve the superior performance over the system with fixed number antenna selection, which will be testified by the following simulation. Although the developed scheme may increase the complexity to some extent, the complexity is relatively lower. It is because we employ the low-complexity approximate BER expressions for BER calculation and comparison, while these expressions are simple linear algebraic calculus (see (30) or (31)), such as addition, multiplication, and division of polynomial. Thus, the total calculation complexity is still relatively lower. More importantly, a good BER performance can be achieved.

5 Simulation results and theoretical evaluation

In this section, the performance of the MIMO-TAS-STBC over quasi-static flat Rayleigh fading channels is evaluated by the derived theoretical formulae and computer simulation. In the evaluation, the Alamouti code (G_2) [24], B_3 and B_4' codes [23] are used for the selective two, three and four transmit antennas, respectively. Gray mapping of bits to symbol is employed. The Monte-Carlo method is used in simulation. For different space-time coding schemes, we will adopt different constellation sizes to maintain the same transmission rate. In evaluating the theoretical performance under perfect CSI, Eqs. (24) and (26) are used for the calculation of BERs of the system using MQAM and MPSK, respectively. Whereas for evaluating the theoretical performance under imperfect CSI, Eqs. (21) and (25) are employed for the calculation of the BERs with MQAM and MPSK, respectively. In the following Figures 1–4, 'xTyRzS' denotes a multiple antenna system with x transmit antennas and y receive antennas as well as z selective antennas.

In Figure 1, we plot the theoretical BERs and simulation results of MIMO-TAS-STBC with 4 transmit antennas and 1 receiver antenna for perfect CSI. When two, three and four transmit antennas are selected, the G_2, B_3 and B_4' codes are employed for STBC. Regarding modulation, 8PSK is used for MIMO with

G_2 and single antenna selection, while 16QAM is used for MIMO with B_3 and B_4' resulting in the overall transmission rate of 3 bit·s^{-1}·Hz^{-1}. The accurate BERs are calculated by Eqs. (24) and (26) for 16QAM and 8PSK, respectively. The approximate BERs are calculated by Eqs. (30) and (31) for 16QAM and 8PSK, respectively. From Figure 1, it is found that the accurate BER can match the simulation very well. Moreover, the approximate BER is also close to the accurate BER, but has lower computational complexity. By comparison, we can see that the 4T1R1S system is superior to 4T1R2S, 4T1R3S and 4T1R4S systems. Although the four systems above can all achieve full diversity (the same slope at high SNR) under perfect CSI according to the diversity gain analysis in Section 4, their coding gains are different leading to different BER performance. Based on the coding gain analysis in Section 4, the single antenna selection system has the coding gain higher than other three systems. Thus, the 4T1R1S system has better performance in the presence of perfect CSI. The above results show that the derived accurate and approximate BER expressions of MIMO-TAS-STBC for perfect CSI are effective.

In Figures 2–4, the performance of MIMO-TAS-STBC with imperfect CSI is evaluated, where 'AAS' denotes the adaptive antenna selection scheme for MIMO-TAS-STBC system. In Figure 2, we plot the theoretical BERs and simulation results of MIMO-TAS-STBC with 4 transmit antennas and 1 receive antenna, where the G_2, B_3 and B_4' codes are employed for STBC for the selective two, three and four transmit antennas, respectively, and the square correlation coefficient c^2=0.9. For G_2 code and single antenna selection, 8PSK is employed, while for B_3 and B_4' code, 16QAM is used. Thus the overall transmission rate is 3 bit·s^{-1}·Hz^{-1}. The accurate BERs are, respectively, calculated by (21) and (25) for 16QAM and 8PSK, and the approximate BERs are calculated by (30) and (31) for 16QAM and 8PSK, respectively. As shown in Figure 2, the accurate BER is in good agreement with the simulation. Moreover, the approximate BER is also close to the accurate BER with lower complexity. Comparing Figures 2 and 1, the BER performance under imperfect CSI is worse than that under perfect CSI because of delayed CSI. Unlike the perfect CSI case for which the system with single antenna selection (i.e., 4T1R1S) has the best performance, 4T1R4S (where all transmit antennas are used) has better performance than other three systems for imperfect CSI, especially at high SNR. It is because the 4T1R4S employs all antennas and does not need CSI to perform antenna selection, while 4T1R3S, 4T1R2S and 4T1R1S need the CSI, but the delayed CSI affects their antenna selection. This result is also verified by the diversity gain analysis in Section 4. For imperfect CSI, the diversity gain of MIMO with all antennas is higher than that with partial antenna selection, and the diversity gains of the systems with more selective antennas are higher than those with fewer selective antennas. Besides, the AAS system outperforms the systems with fixed number antenna selection obviously. This is because the former can perform adaptive antenna selection according to the CSI feedback, while for the latter, the antenna selection is fixed and cannot adapt to the CSI change.

In Figure 3, we plot the theoretical BERs and simulation results of MIMO-TAS-STBC with 4 transmit antennas and 2 receive antennas, where the G_2, B_3 and B_4' codes are employed for STBC for the selective two, three and four transmit antennas, respectively, and the square correlation coefficient $c^2 = 0.8$. Regarding modulation, 8PSK is used for 4T2R1S and 4T2R2S, while 16QAM is used for 4T2R3S and 4T2R4S resulting in the overall transmission rate of 3 bit·s^{-1}·Hz^{-1}. The accurate and approximate BER formulae of MQAM are, respectively, given by (21) and (30), and the accurate and approximate BER formulae of MPSK are, respectively, given by (25) and (31). It is found that the accurate BER can match the simulation very well. Moreover, the approximate BER is also close to the accurate BER, but has lower complexity. Besides, the results similar to Figure 2 can be observed. Namely, the system with adaptive TAS has better performance than that with fixed TAS. For the systems with fixed TAS at high SNR, 4T2R4S outperforms the 4T2R3S, 4T2R2S and 4T2R1S, 4T2R3S outperforms 4T2R2S and 4T2R1S, and 4T2R2S outperforms 4T2R1S. The above results further show that the provided diversity gain analysis is valid, and the derived accurate and approximate BER expressions under imperfect CSI are also effective.

In Figure 4, we investigate the effects of correlation coefficient on the BER performance of MIMO-TAS-STBC under imperfect CSI, where 8PSK and 16QAM are employed for the modulations yielding the overall transmission rate of 3 bit·s^{-1}·Hz^{-1}. The system configuration is the same as that of

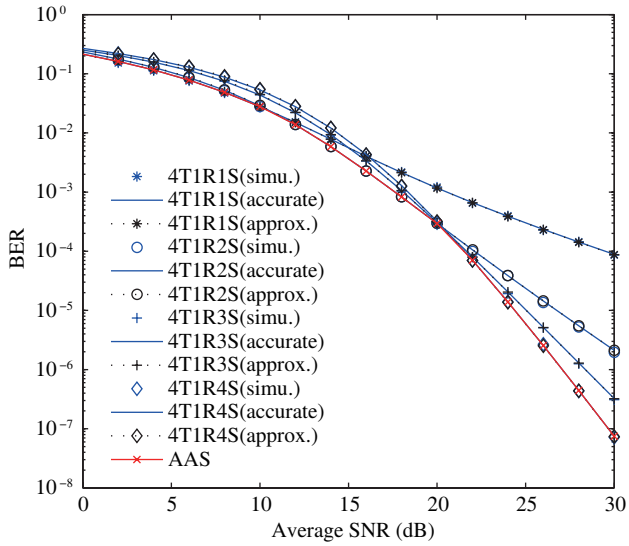

Figure 2 (Color online) BER of MIMO-TAS-STBC with 4 transmit antennas and 1 receive antenna under imperfect CSI.

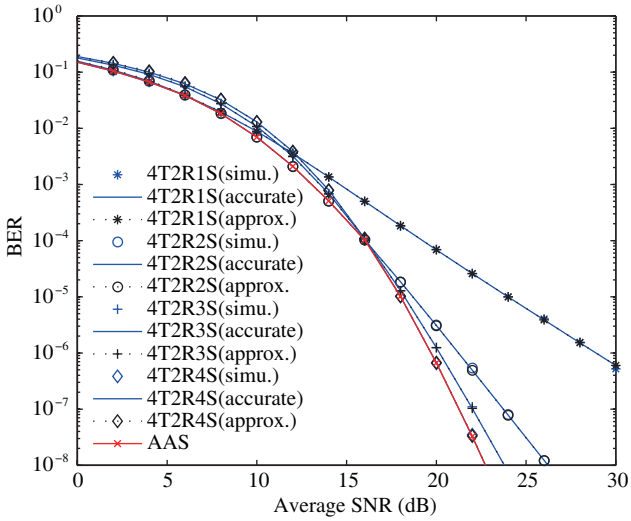

Figure 3 (Color online) BER of MIMO-TAS-STBC with 4 transmit antennas and 2 receive antennas under imperfect CSI.

Figure 3. In Figure 4, we plot the BER versus the correlation coefficient for average SNR = 15 dB. From the figure, we find that the 4T2R1S with one selective antenna is superior to the other comparative systems for large correlation coefficient c (corresponding to small time delay) due to better coding gain. However, for small c (corresponding to large time delay), especially when the correlation coefficient c is below 0.85, the performance of 4T2R1S system is degraded more seriously than the other systems. Moreover, with correlation coefficient c being small, the system with more selective antennas is superior to that with fewer selective antennas. Namely, 4T2R2S outperforms 4T2R1S, 4T2R3S outperforms 4T2R2S, and 4T2R4S outperforms 4T2R3S as the value of c increasingly decreasing. This is because the CSI feedback becomes more unreliable at low correlation, and the resulting selective antennas are not optimal. Thus, the system performance with fewer selective antennas will be worse. Besides, our AAS system still obtains better BER performance than other non-adaptive systems.

6 Conclusion

Based on imperfect CSI caused by delayed feedback, the performance of MIMO system with arbitrary number antenna selection and STBC has been studied. The MGF and PDF of effective SNR of the

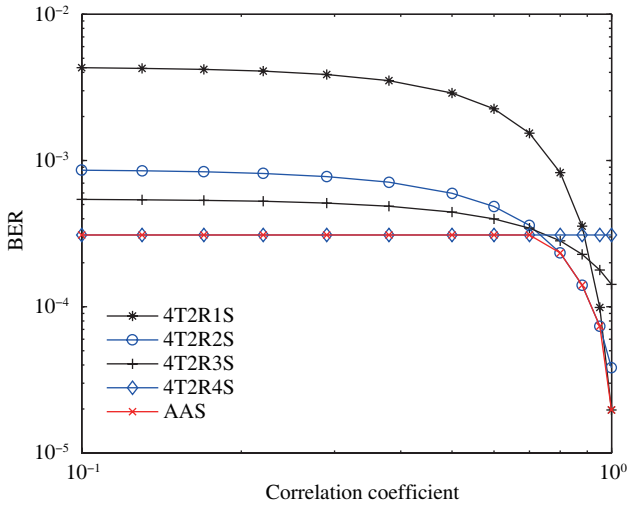

Figure 4 (Color online) Effect of correlation coefficient on BER of MIMO-TAS-STBC.

systems are derived. According to these results, and using mathematical manipulation, the accurate and approximate BER expressions for perfect and imperfect CSI are obtained. The accurate BER expressions can match the simulation results well. Also the approximate BER curves are very close to the accurate ones. Thus, these expressions can provide good performance evaluation for MIMO-TAS-STBC systems in fading channel, and avoid the conventional requirement for numerical integration or Monte Carlo simulation. With the approximate BER expressions, upper and lower bounds of BER are provided. Based on the upper and lower bounds of BER, the diversity gain and coding gain of the system at high SNR are analyzed. It is shown that the MIMO-TAS-STBC with K selected transmit antennas can achieve full diversity order of MN for perfect CSI, and partial diversity gain of KN for imperfect CSI. Besides, an adaptive antenna selection scheme is also developed in terms of approximate BER expressions. With this scheme, the system can obtain superior performance over that with the conventional fixed number antenna selection scheme. Simulation results illustrate the effectiveness of the presented theoretical analysis.

Acknowledgements This work was supported in part by National Natural Science Foundation of China (Grant Nos. 61172077, 61571225), Qing Lan Project of Jiangsu, City University of Hong Kong (Grant No. 7002763), and Shenzhen Strategic Emerging Industry Development Funds (Grant No. JSGG20150331160845693).

Conflict of interest The authors declare that they have no conflict of interest.

References

1 Tarokh V, Seshadri N, Calderbank A R. Space-time codes for high data rate wireless communication: performance criterion and code construction. IEEE Trans Inform Theory, 1999, 44: 744–765
2 Guey J C, Fitz M P, Bell M R, et al. Signal design for transmitter diversity wireless communication systems over Rayleigh fading channels. IEEE Trans Commun, 1999, 47: 527–537
3 Tarokh V, Jafarkhani H, Calderbank A R. Space-time block codes from orthogonal designs. IEEE Trans Inform Theory, 1999, 45: 1456–1467
4 Win M Z, Winters J H. Analysis of hybrid selection/maximal-ratio combining in Rayleigh fading. IEEE Trans Commun, 1999, 47: 1773–1776
5 Thoen S, van der Perre L, Gyselinckx B, et al. Performance analysis of combined transmit-SC/receive-MRC. IEEE Trans Commun, 2001, 49: 5–8
6 Chen Z, Yuan J, Vucetic B. Analysis of transmit antenna selection/ maximal-ratio combing in Rayleigh fading channel. IEEE Trans Veh Tech, 2005, 54: 1312–1321
7 Yang N, Yeoh P L, Elkashlan M, et al. Cascaded TAS/MRC in MIMO multiuser relay networks. IEEE Trans Wirel Commun, 2012, 11: 3829–3839
8 Yang N, Yeoh P L, Elkashlan M, et al. Transmit antenna selection for security enhancement in MIMO wiretap channels. IEEE Trans Commun, 2013, 61: 144–154
9 Yang L, Qin L. Performance of Alamouti scheme with transmit antenna selection for M-ary signals. IEEE Trans Wirel Commun, 2006, 5: 3365–3369

10 Coskun A F, Kucur O, Altunbas I. Performance analysis of space-time block codes with transmit antenna selection in Nakagami-m fading channels. Wirel Pers Commun, 2012, 67: 557–571
11 Molisch A F, Win M Z, Winters J H. Reduced-complexity transmit/receive-diversity systems. IEEE Trans Signal Process, 2003, 51: 2729–2738
12 Molisch A F, Win M Z. MIMO systems with antenna selection. IEEE Microw Mag, 2004, 5: 46–56
13 Kaviani S, Tellambura C. Closed-form BER analysis for antenna selection using orthogonal space-time block codes. IEEE Commun Lett, 2006, 10: 704–706
14 Zhang W, Tellambura C. Performance analysis of joint transmit and receive antenna selection with orthogonal space-time coding. IEEE Trans Veh Tech, 2010, 59: 2631–2635
15 Lee D, Jeong B J. Performance analysis of scheduled cognitive radio systems with MIMO transmission. IEEE Trans Veh Tech, 2013, 62: 4088–4093
16 Yu X B, Dang X Y, Leung S H, et al. Unified analysis of multiuser scheduling for downlink MIMO systems with imperfect CSI. IEEE Trans Wirel Commun, 2014, 13: 1344–1355
17 Coskun A F, Kucur O. Analysis of diversity schemes employing antenna selection in the presence of channel estimation errors and feedback delay. Wirel Commun Mob Comput, 2016, 16: 300–312
18 Phan K T, Tellambura C. Capacity analysis for transmit antenna selection using orthogonal space-time block codes. IEEE Commun Lett, 2007, 11: 423–425
19 Ma Y, Chai C C. Unified error probability analysis for generalized selection combining in Nakagami fading channels. IEEE J Select Areas Commun, 2000, 18: 2198–2210
20 Bahceci I, Duman T M, Altunbasak Y. Antenna selection for multiple-antenna transmission systems: performance analysis and code construction. IEEE Trans Inform Theory, 2003, 49: 2669–2681
21 Zhu H. Performance comparison between distributed antenna and microcellular systems. IEEE J Select Areas Commun, 2011, 29: 1151–1163
22 Wang J, Zhu H, Gomes N J. Distributed antenna systems for mobile communications in high speed trains. IEEE J Select Areas Commun, 2012, 30: 675–683
23 Lu K, Fu S, Xia X G. Closed-form designs of complex orthogonal space-time block codes of rates (k+1)/(2k) for 2k-1 or 2k transmit antennas. IEEE Trans Inform Theory, 2005, 51: 4340–4347
24 Tarokh V, Jafarkhani H, Calderbank A R. Space-time block coding for wireless communications: performance results. IEEE J Select Areas Commun, 1999, 17: 451–460
25 Proakis J G. Digital Communications. 4th ed. New York: McGraw-Hill, 2001
26 David H A. Order Statistics. 2nd ed. New York: Wiley, 1981
27 Sharma V, Premkumar K, Swamy R N. Exponential diversity achieving spatio-temporal power allocation scheme for fading channels. IEEE Trans Inform Theory, 2008, 54: 188–208
28 Yu X B, Leung S H, Kuang Q, et al. Performance analysis of variable-power adaptive modulation with outdated feedback for space-time coded MIMO systems. IEEE Trans Veh Tech, 2012, 61: 2613–2624
29 Gradshteyn I S, Ryzhik I M. Table of Integrals, Series, and Products. 7th ed. Pittsburgh: Academic Press, 2007
30 Alouini M S, Goldsmith A J. Adaptive modulation over Nakagami fading channels. Wirel Pers Commun, 2000, 13: 119–143
31 Cho K, Yoon D. On the general BER expression of one-and two-dimensional amplitude modulations. IEEE Trans Commun, 2002, 50: 1074–1080
32 Simon M K, Alouini M S. Digital Communication Over Fading Channels: a Unified Approach to Performance Analysis. New York: Wiley, 2000
33 Lu J, Letaief K B, Chuang J C I, et al. M-PSK and M-QAM BER computation using signal-space concepts. IEEE Trans Commun, 1999, 47: 181–184
34 Loskot P, Beaulieu N C. Prony and polynomial approximations for evaluation of the average probability of error over slow-fading channels. IEEE Trans Veh Tech, 2009, 58: 1269–1280
35 Zheng L, Tse D. Diversity and multiplexing: a fundamental tradeoff in multiple antenna channels. IEEE Trans Inform Theory, 2003, 49: 1073–1096

Appendix A

In this appendix, we will derive the upper and lower bound of MGF of $\hat{\rho}$, $\Psi_{\hat{\rho}}(s)$ given in (9) and (10) based on the following Lemma.

Lemma

$$\mathrm{e}^{-x}\frac{x^n}{n\,!} \leqslant 1-\mathrm{e}^{-x}\sum_{i=0}^{n-1}\frac{x^i}{i\,!} \leqslant \frac{x^n}{n\,!}, x>0. \tag{A1}$$

The proofs of the first and second inequalities of Lemma are, respectively, shown in Lemma 1 and Lemma 2 of [20].

Firstly, the upper bound is derived. With the second inequality in (A1) and (3), the CDF of $\hat{\rho}_k$ $(k=1,\ldots,K)$ can be changed to

$$F_{\hat{\rho}_k}(x)=\Phi(N,x/\bar{\rho}')=1-\mathrm{e}^{-x/\bar{\rho}'}\sum_{n=0}^{N-1}(x/\bar{\rho}')^n/n! \leqslant (x/\bar{\rho}')^N/N!, \quad k=1,\ldots,K, \tag{A2}$$

where $\Phi(m,z)=\int_0^z t^{m-1}\mathrm{e}^{-t}/\Gamma(m)\mathrm{d}t$ is the normalized incomplete Gamma function [29]. Thus, with (4), (2) and (A2),

the MGF $\Psi_{\hat{\rho}}(s)$ in (7) can be re-expressed as

$$\begin{aligned}\Psi_{\hat{\rho}}(s) &= K!\binom{M}{K}\int_0^{\infty}\mathrm{e}^{-sx_1}f_{\hat{\rho}_1}(x_1)\int_0^{x_1}\mathrm{e}^{-sx_2}f_{\hat{\rho}_2}(x_2)\cdots\int_0^{x_{K-2}}\mathrm{e}^{-sx_{K-1}}f_{\hat{\rho}_{K-1}}(x_{K-1})\\ &\quad\times\int_0^{x_{K-1}}\mathrm{e}^{-sx_K}[F_{\hat{\rho}_K}(x_K)]^{M-K}f_{\hat{\rho}_K}(x_K)\mathrm{d}x_K\mathrm{d}x_{K-1}\cdots\mathrm{d}x_2\mathrm{d}x_1\\ &\leqslant K!\binom{M}{K}\int_0^{\infty}\mathrm{e}^{-sx_1}f_{\hat{\rho}_1}(x_1)\int_0^{x_1}\mathrm{e}^{-sx_2}f_{\hat{\rho}_2}(x_2)\cdots\int_0^{x_{K-2}}\mathrm{e}^{-sx_{K-1}}f_{\hat{\rho}_{K-1}}(x_{K-1})\\ &\quad\times\frac{N\bar{\rho}'^{NK-NM-N}}{(N!)^{M-K+1}}\int_0^{x_{K-1}}\mathrm{e}^{-(s+1/\bar{\rho}')x_K}x_K^{MN-KN+N-1}\mathrm{d}x_K\mathrm{d}x_{K-1}\cdots\mathrm{d}x_2\mathrm{d}x_1.\end{aligned}\tag{A3}$$

Substituting (A2) into (A3) gives

$$\begin{aligned}\Psi_{\hat{\rho}}(s) &\leqslant \int_0^{\infty}\mathrm{e}^{-sx_1}f_{\hat{\rho}_1}(x_1)\int_0^{x_1}\mathrm{e}^{-sx_2}f_{\hat{\rho}_2}(x_2)\cdots\int_0^{x_{K-2}}f_{\hat{\rho}_{K-1}}(x_{K-1})\\ &\quad\times\mathrm{e}^{-sx_{K-1}}M!(x_{K-1}/\bar{\rho}')^{NM-NK+N}/[(M-K+1)!(N!)^{M-K+1}]\mathrm{d}x_{K-1}\cdots\mathrm{d}x_2\mathrm{d}x_1\\ &= \frac{M!N}{(M-K+1)!(N!)^{M-K+2}}\int_0^{\infty}\mathrm{e}^{-sx_1}f_{\hat{\rho}_1}(x_1)\int_0^{x_1}\mathrm{e}^{-sx_2}f_{\hat{\rho}_2}(x_2)\cdots\int_0^{x_{K-3}}\mathrm{e}^{-sx_{K-2}}f_{\hat{\rho}_{K-2}}(x_{K-2})\\ &\quad\times\frac{\Gamma(NM-NK+2N)}{(s\bar{\rho}'+1)^{NM-NK+2N}}\Phi(MN-KN+2N,(s+1/\bar{\rho}')x_{K-2})\mathrm{d}x_{K-2}\cdots\mathrm{d}x_2\mathrm{d}x_1\\ &= \Gamma(MN+1){}_2F_1(1,MN,MN-N+1,0.5)/[(N!)^M(s\bar{\rho}'+1)^{NM}2^{NM}],\end{aligned}\tag{A4}$$

where the equation $\int_0^{\infty}t^{u-1}\mathrm{e}^{-\alpha t}\Phi(v,\beta t)\mathrm{d}t=\frac{\beta^v\Gamma(u+v)}{\Gamma(v+1)(\alpha+\beta)^{u+v}}{}_2F_1(1,u+v,v+1,\frac{\alpha}{\alpha+\beta})$ [29] is utilized, and ${}_2F_1(x,y,w,z)$ is the Gaussian hypergeometric function. Detailed derivation is omitted due to the limited space. With (A4), the upper bound of the MGF $\Psi_{\hat{\rho}}(s)$ can be attained, which is also shown as (9).

Similar to the above analysis method for upper bound, using the first inequality of Lemma, we can obtain the lower bound of the MGF, $\Psi_{\hat{\rho}}(s)$, i.e.,

$$\Psi_{\hat{\rho}}(s)\geqslant\Psi_{\hat{\rho}}^{(l)}(s)=\frac{\Gamma(NM+1)}{(N!)^M(M+K\bar{\rho}'s)^{NM}}{}_2F_1\left(1,NM,NM-N+1,\frac{(K-1)\bar{\rho}'s+M-1}{K\bar{\rho}'s+M}\right).\tag{A5}$$